Electronic Supporting Information

Solid Polymer Electrolyte of Ionic Liquids via Bicontinuous Ion Transport Channel for Lithium Metal Batteries

Won-Jang Cho,[a‡] Seok-Kyu Cho,[b‡] Jun Hyuk Lee,[c] Jeong Hoon Yoon,[a] Sangwoo Kwon,[d] Chanui Park,[d] Won Bo Lee,[d] Pil J. Yoo,[c,g] Minjae Lee,[e] Sungkyun Park,[f] Tai Hui Kang[c] and Gi-Ra Yi*[a]

[a]Department of Chemical Engineering, Pohang University of Science and Technology (POSTECH), Pohang 37673, Republic of Korea.

[b]UBATT Inc., Daejeon 34036, Republic of Korea.

[c]School of Chemical Engineering, Sungkyunkwan University (SKKU), Suwon 16419, Republic of Korea.

[d]School of Chemical and Biological Engineering, Institute of Chemical Processes, Seoul National University, Seoul 08826, Republic of Korea.

[e]Department of Chemistry, Kunsan National University, Gunsan 54150, Republic of Korea.

[f]Department of Physics, Pusan National University, Busan 46241, Republic of Korea.

[g]SKKU Institute of Energy Science and Technology (SIEST), Sungkyunkwan University (SKKU), Suwon 16419, Republic of Korea.

*Corresponding author: yigira@postech.ac.kr

‡W.-J. C. and S.-K. C. contributed equally to this work.

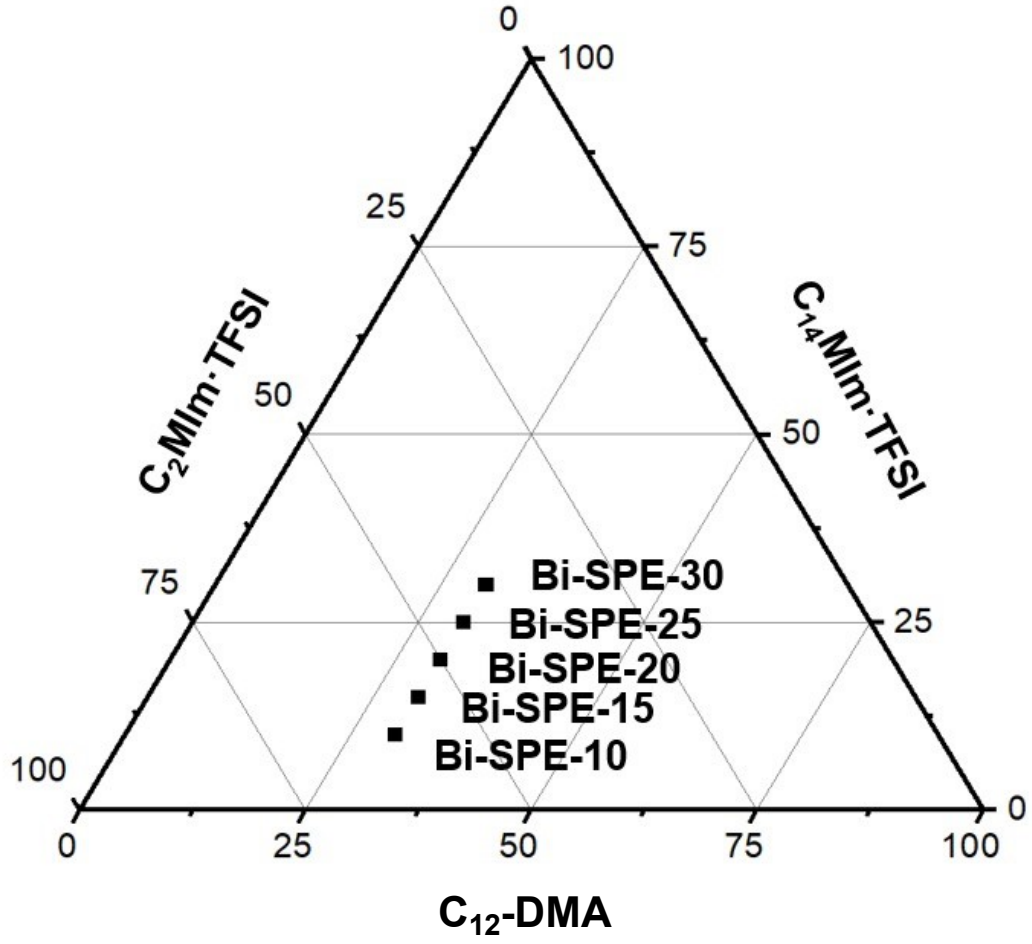

Figure S1. Ternary diagram of C_2Mim·TFSI, C_{14}Mim·TFSI, and C_{12}-DMA for Bi-SPE series.

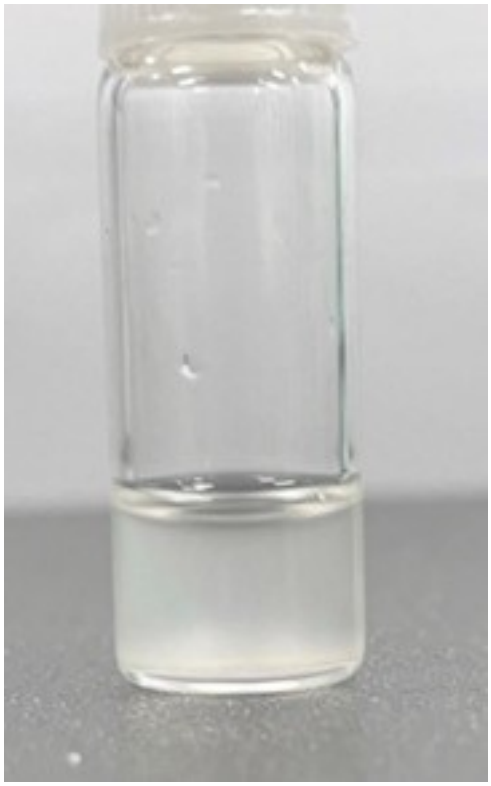

Figure S2. Digital image of Bi-SPE-5, which is opaque, indicating that thermodynamically unstable macroemulsions were formed.

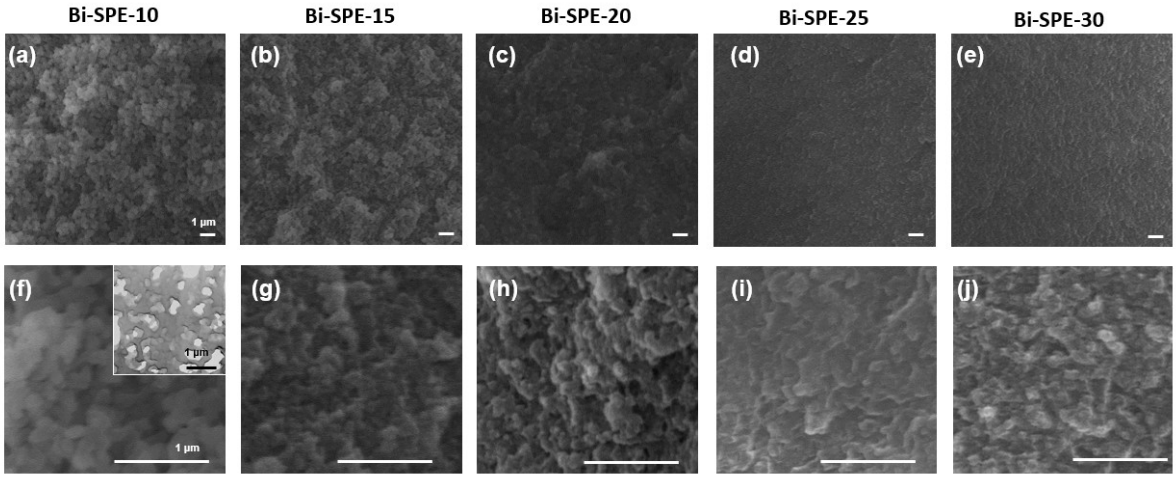

Figure S3. (a-e) Low- and (f-j) high-magnification scanning electron microscopy (SEM) images of (a,f) Bi-SPE-10, (b,g) Bi-SPE-15, (c,h) Bi-SPE-20, (d,i) Bi-SPE-25, and (e,j) Bi-SPE-30. Inset of (f) shows the cross-sectional TEM image of Bi-SPE-10. Scale bars are 1µm.

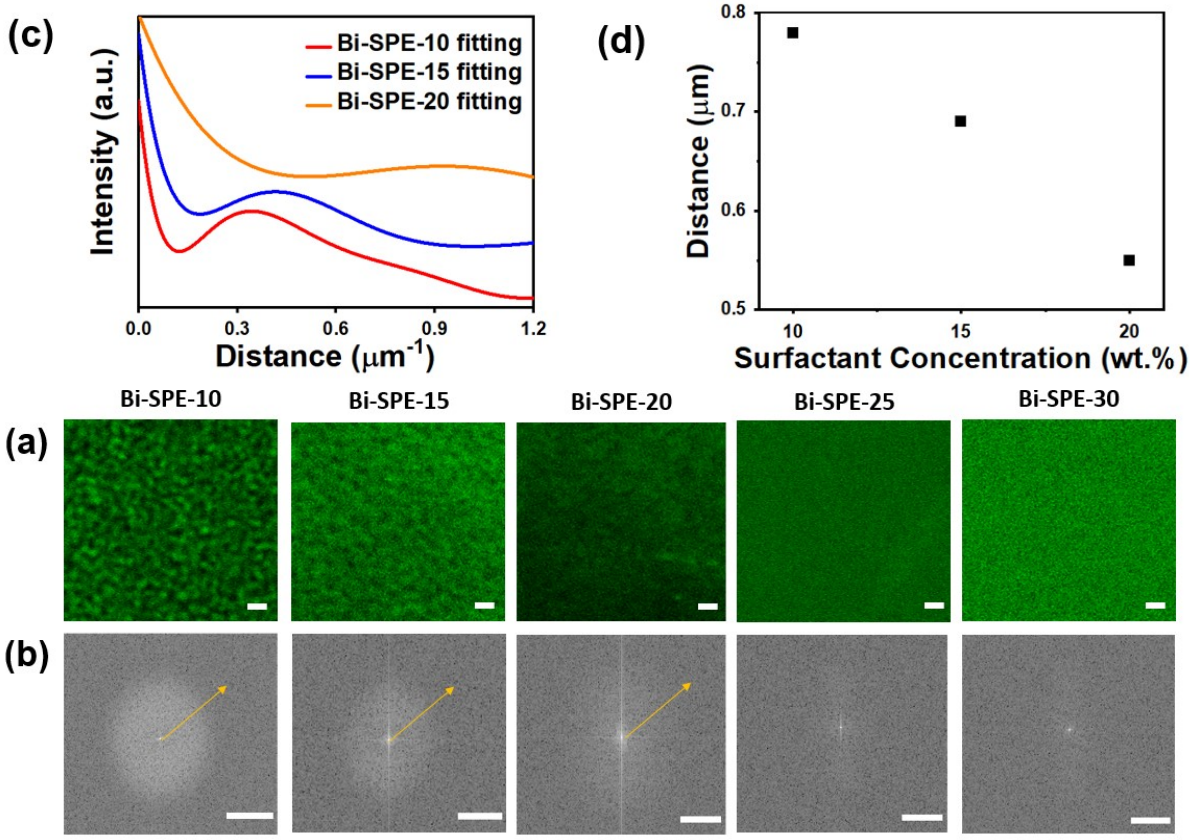

Figure S4. (a) Confocal microscopy images of the Bi-SPE series with green-colored solidified C12-DMA (scale bar = 1μm). (b) FFT images from confocal microscopy (scale bar = 0.5μm^{-1}). (c) Line intensities along the yellow arrows in FFT images of Bi-SPE-10, -15, -20. (d) Interdistances domain of Bi-SPE-10, -15, -20.

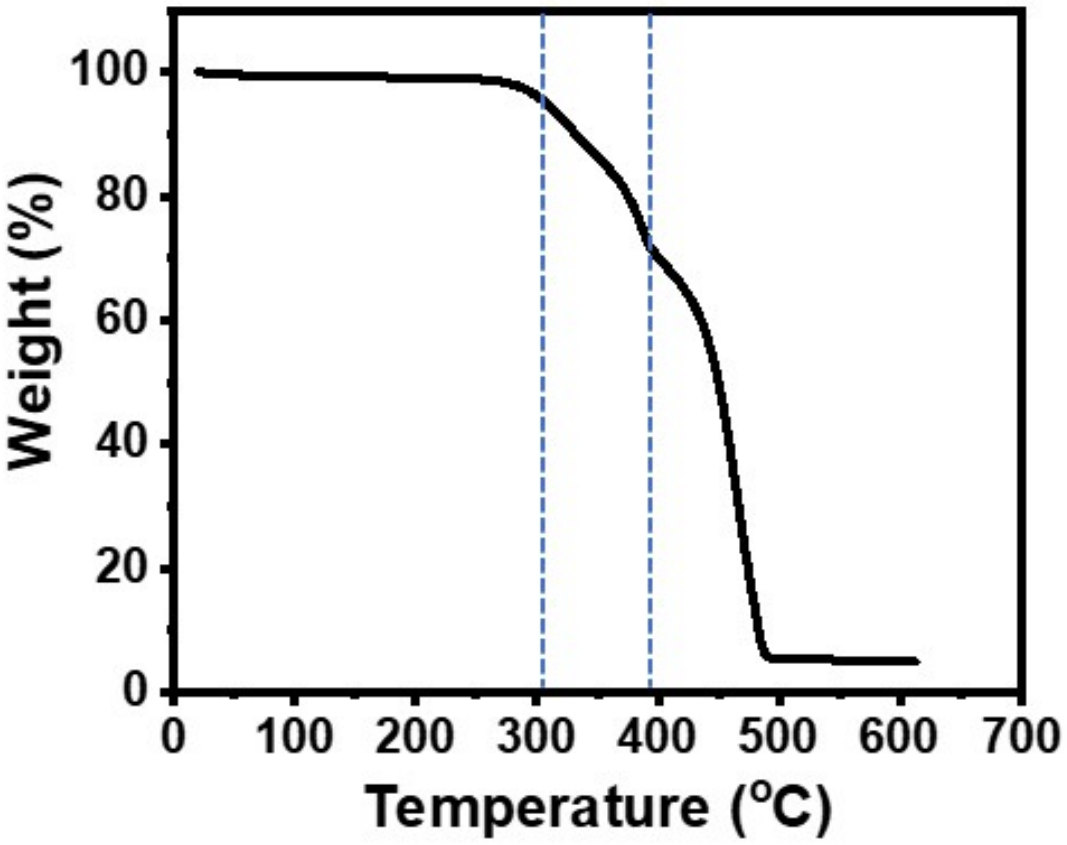

Figure S5. TGA curve of Bi-SPE-10.

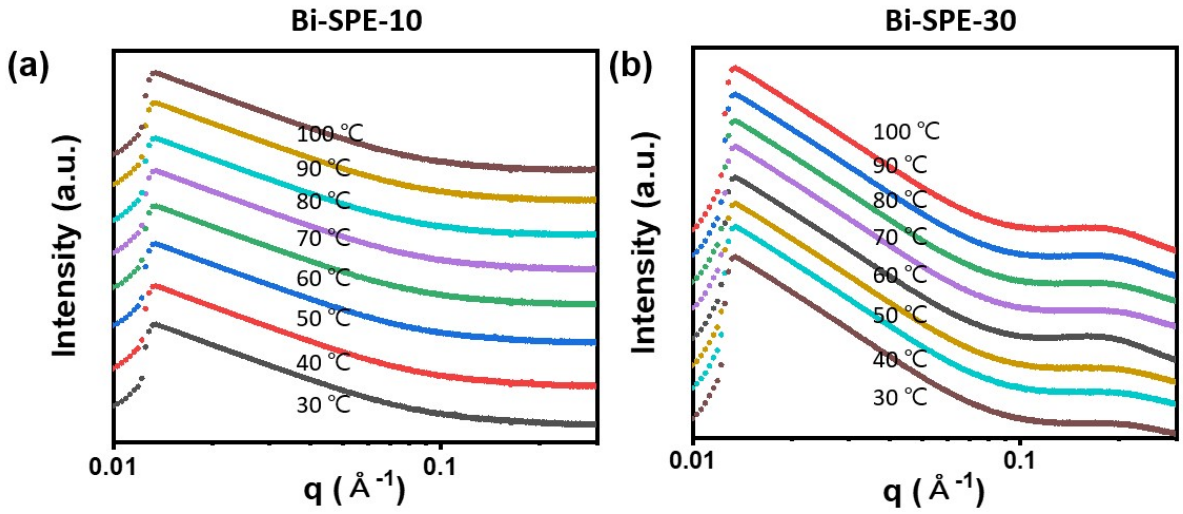

Figure S6. SAXS fitting curves with the function of temperature from 30 to 100 ℃.

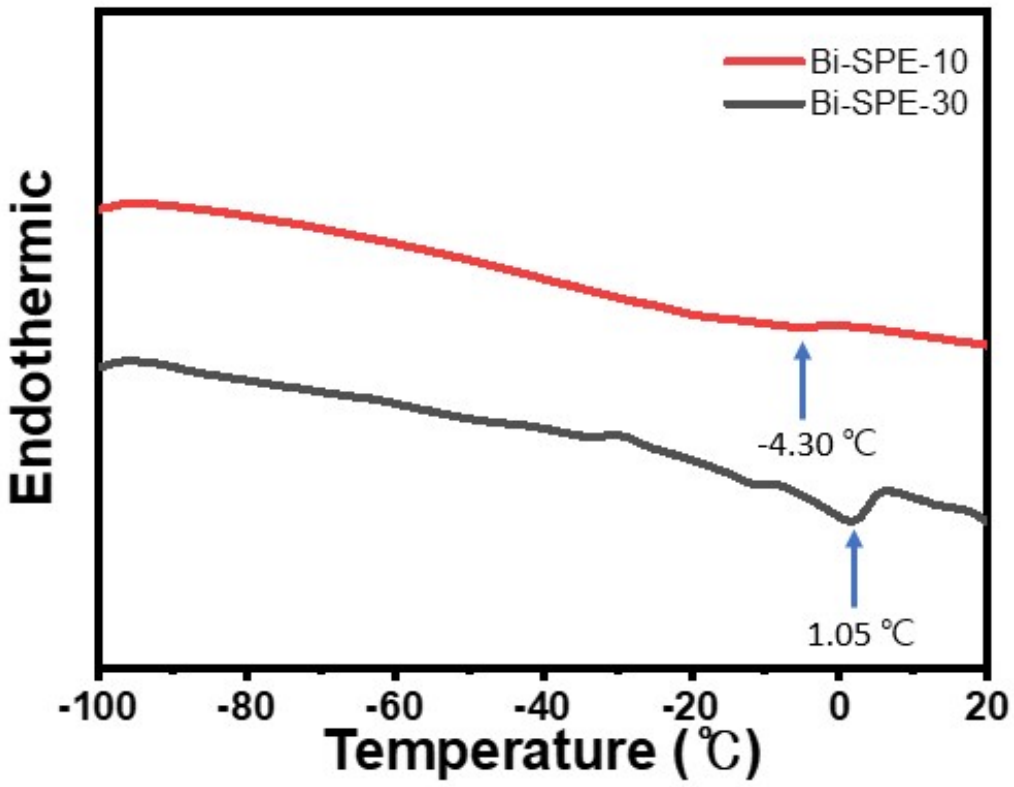

Figure S7. DSC curves of Bi-SPE-10 and Bi-SPE-30.

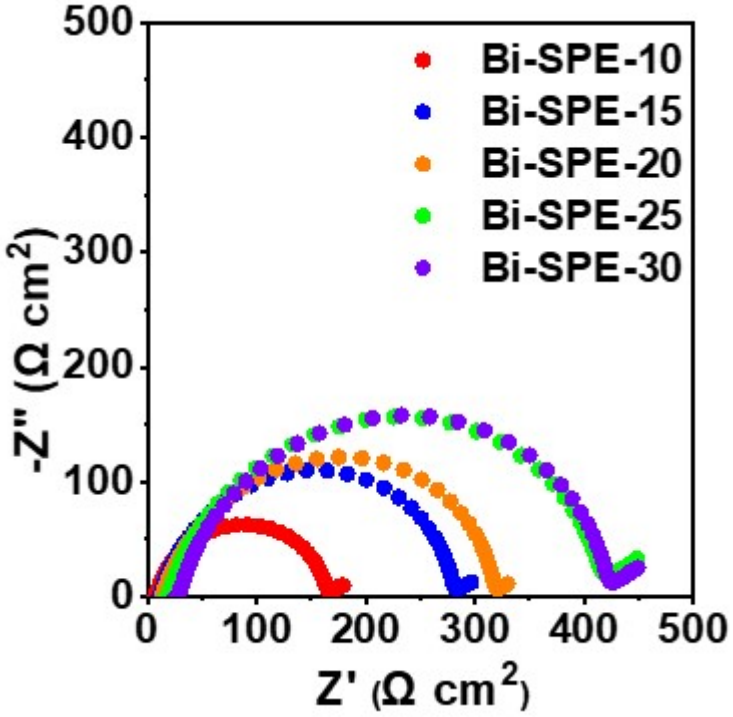

Figure S8. Impedance of symmetric lithium cell with five Bi-SPEs after steady-state.

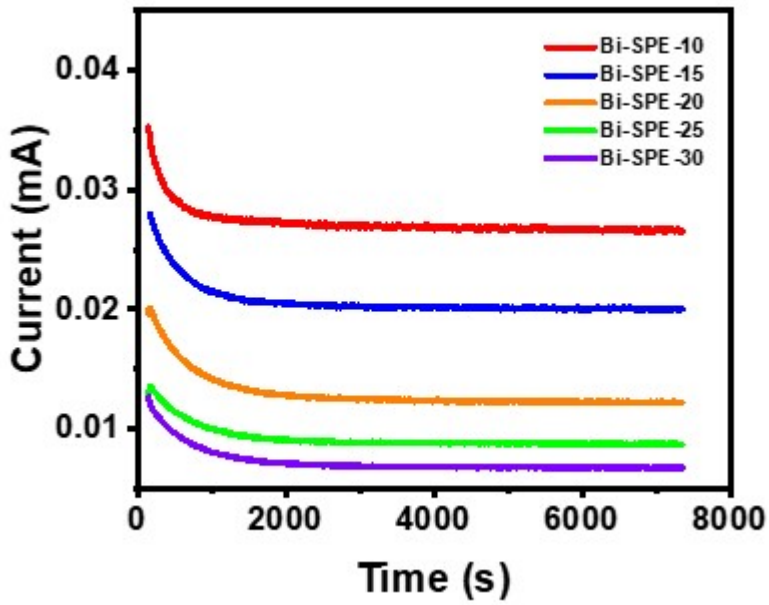

Figure S9. Time-dependent current profiles at 10 mV of symmetric lithium cells with five Bi-SPEs.

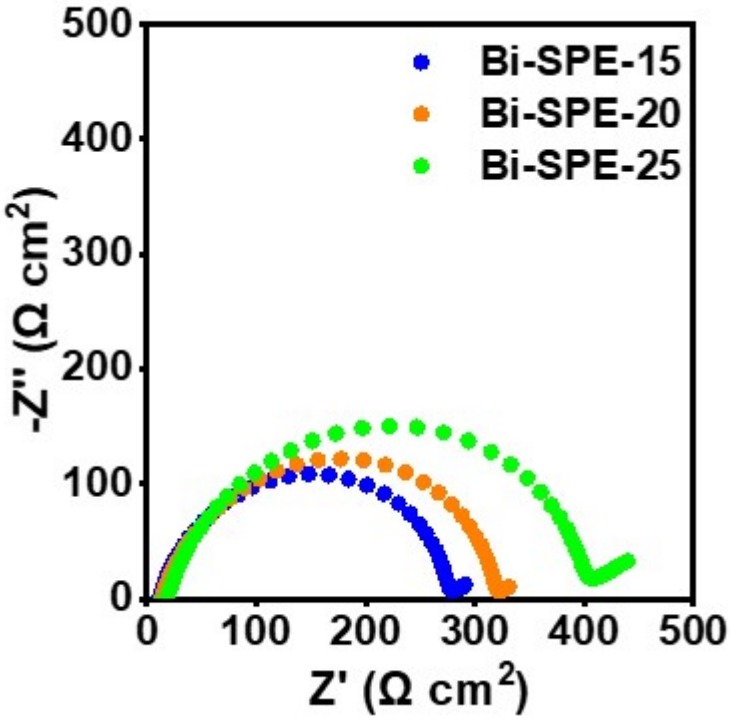

Figure S10. Impedance spectra of symmetric lithium cells with Bi-SPE-15, -20 and -25 before steady-state.

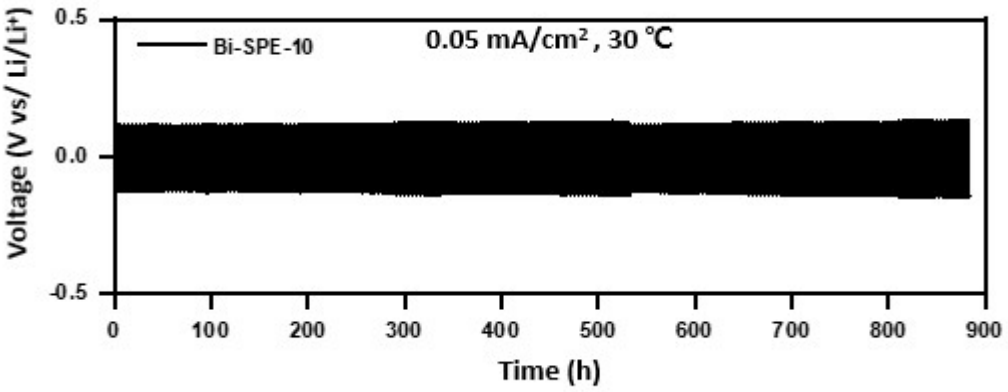

Figure S11. Time-dependent voltage profile of Li|Bi-SPE-10|Li symmetric cell at 0.05 mA/cm^2

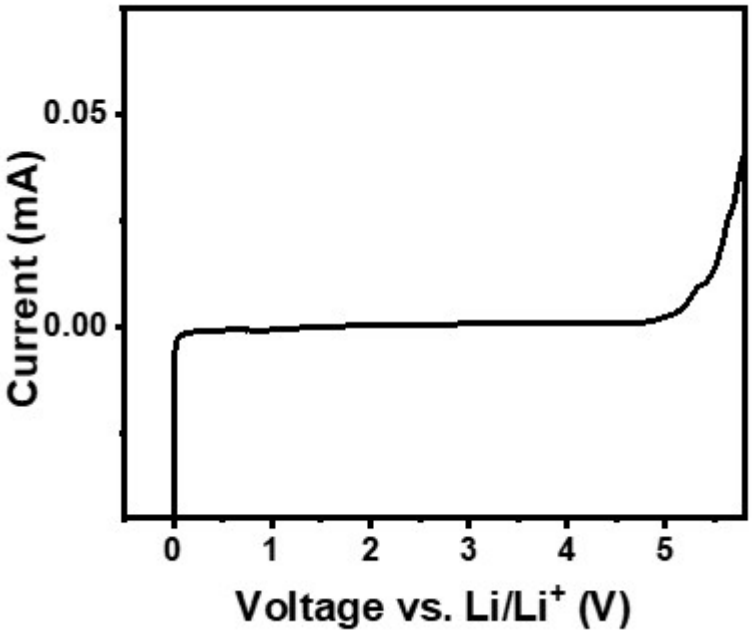

Figure S12. Linear sweep voltammogram of Bi-SPE-10.

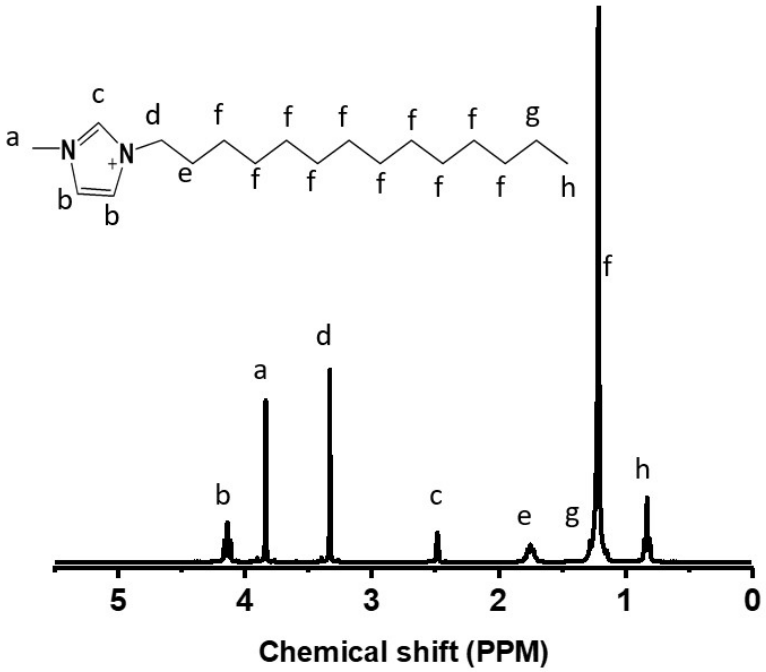

Figure S13. 1H NMR spectrum of C_{14}MIm·Cl with corresponding assignment of the signals of imidazolium unit and aliphatic chain.

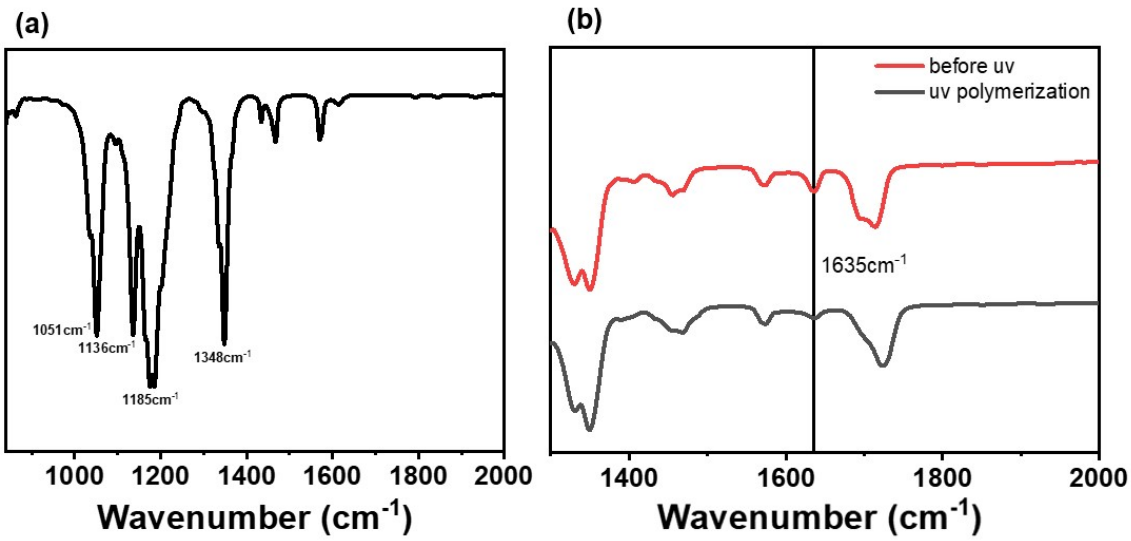

Figure S14. FT-IR peaks of (a) C_{14}MIm·TFSI and (b) Bi-SPE-10 before and after UV polymerization, in which the peak of C=C in acrylate monomers decreased at 1635 cm^{-1}.

Table S1. Initial and equilibrium impedances (R_o, R_{ss}), initial and equilibrium currents (I_o, I_{ss}), and Lithium transference number (t_+) of five Bi-SPEs.

Sample name	R_o (ohm)	R_{ss} (ohm)	I_o (mA)	I_{ss} (mA)	t_+
Bi-SPE-10	165.0	165.8	0.035	0.0265	0.58
Bi-SPE-15	275.2	279.2	0.027	0.021	0.48
Bi-SPE-20	311	311.7	0.019	0.012	0.42
Bi-SPE-25	388.3	410.3	0.016	0.01	0.39
Bi-SPE-30	407.4	430.2	0.018	0.0067	0.35